



OPEN

A novel univariate legendre polynomial method for probabilistic failure load prediction in composite open-hole laminate

Mingxuan Li, Ben Yuan, Fugui Li, Yuan Fang & Xiaolei Zhu✉

A novel univariate Legendre polynomial method is proposed for probabilistic failure load prediction in composite open-hole laminate based on the dimension-reduction method and Legendre polynomial. The effectiveness of the method was verified by comparison with experimental results. The mean prediction error was less than 3%, and the coefficient of variation of the prediction error was less than 15%, indicating that the new method can effectively predict the probabilistic failure load of composite open-hole laminate. In addition, ULAM was compared with RSM and Kriging model to verify its superiority. Given the same number of sample points, ULAM achieved higher prediction accuracy than the other two models. Finally, the effect of the polynomial order on the prediction accuracy of ULAM was investigated. If the order is too low, underfitting will occur. While increasing the order can improve the prediction accuracy, an excessively high order leads to overfitting, which in turn degrades the model's performance.

Keywords Composite open-hole laminate, Legendre polynomial, Dimension reduction method, Probabilistic, Prediction

The fiber-reinforced composite is widely used in aerospace, transportation and other fields owing to the advantages of light weight, high specific strength, high specific stiffness, fatigue resistance and designability¹⁻³. In the actual application process, the composite structure is often necessary to open holes for the requirement of structural function and connection between components. However, due to the uncertainty of the manufacturing processes and material parameters, the mechanical properties of composite open-hole laminate are dispersed moderately, which endangers the safety and reliability of the composite structure^{4,5}. However, the traditional safety factor method cannot quantify the probability of failure risk and is also difficult to fully tap the potential of material performance. Probability analysis methods can directly quantify the failure probability of structures under uncertainty, thereby providing a theoretical basis for reliability optimization design and achieving a balance between safety and economy⁶. Therefore, the probabilistic analysis method should be used to predict the strength of the composite open-hole plate to guarantee its safety in actual application process^{7,8}.

Monte Carlo Simulation (MCS) is a well-established and frequently used technique for probabilistic analysis. Wan et al.⁹ predicted the damage progression and strength probability distribution of composite laminates based on MCS. Lubritz et al.¹⁰ utilized MCS to investigate the influence of microscopic mechanical property parameters on the tensile properties of composite laminated plates. The calculation results show that this method is applicable to calculating the average and standard deviation of most linear material parameters of the studied carbon fiber-reinforced polymer (CFRP). Tang et al.¹¹ conducted a detailed probability analysis based on multi-scale uncertainty propagation to quantify the failure probability of the design criterion relative to the static damage initiation and the prestressed vibration resonance margin. The failure probability of the damage initiation of the composite laminate was predicted using MCS. Mukherjee et al.¹² studied the effect of material parameter uncertainty on the design of laminated composite using MCS. However, MCS suffers from high computational cost. To improve efficiency, scholars have adopted moment methods to solve uncertainty problems. Lin et al.¹³ studied the probabilistic failure of laminate composite plates based on the first-order second moment method. However, even a small error in the probability density function will lead to poor accuracy. Surrogate models were introduced for probabilistic analysis of composites to improve the calculation accuracy¹⁴. Zhou and Haeri et al.^{15,16} carried out the reliability and sensitivity of composite structures using the adaptive Kriging surrogate

School of Mechanical and Power Engineering, Nanjing Tech University, Nanjing 211816, China. ✉email: zhuxiaolei@njtech.edu.cn

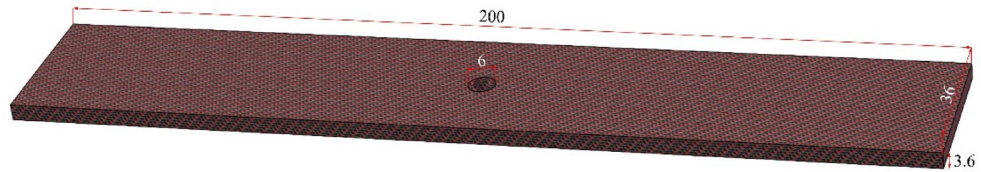


Fig. 1. The configuration of composite open-hole laminate.

Parameter		Mean	Standard deviation	Distribution
Elastic modulus (GPa)	E_{11}	125	6.25	Normal
	$E_{22} = E_{33}$	8.193	0.40965	Normal
Poisson's ratio	$\nu_{12} = \nu_{13}$	0.3	-	-
	ν_{23}	0.4	-	-
Shear modulus (GPa)	$G_{12} = G_{13}$	3.307	0.16535	Normal
	G_{23}	3.151	0.15755	Normal
Tensile strength (MPa)	X_T	1600	80	Normal
	$Y_T = Z_T$	25	1.25	Normal
Comprehensive strength (MPa)	X_C	592	-	-
	$Y_C = Z_C$	98	-	-
Shear strength (MPa)	$S_{12} = S_{13}$	53	2.65	Normal
	S_{23}	38	1.9	Normal

Table 1. Statistical characteristics of random variables.

model. Soares et al.^{17,18} adopted response surface method to study the failure probability of composite plates under low-velocity impact account for the uncertainties of material properties and initial impact velocity. Carrere et al.¹⁹ studied the effect of the uncertainty parameter on the composite structure using response surface method. When the surrogate models are used to deal with high $F = G(\mathbf{x}) = G(x_1, x_2, \dots, x_n)$ h-dimensional nonlinear problems, a large number of sample points are required to obtain higher prediction accuracy. Li and Qiu et al.^{20,21} used a novel uncertainty analysis method based on the polynomial to assess the reliability of composite materials, which lacked experimental validation.

In conclusion, the calculation accuracy of the existing probability analysis methods when dealing with high-dimensional nonlinear problems is closely related to the number of sample points. Although the prediction accuracy can meet the engineering requirements, the calculation cost is huge. Therefore, it is highly necessary to establish a prediction model that requires only a small number of sample points without reducing accuracy. In this paper, a probabilistic failure load prediction method for composite open-hole laminate was proposed combining the dimension reduction method (DRM) and Legendre polynomial (LP). Considering the uncertainty of material parameters, a univariate Legendre approximation model (ULAM) is established. To verify the correctness of the model, static tensile experiments were carried out on composite open-hole laminates, and the ultimate loads were obtained. The predicted results were compared with the experimental results to verify the effectiveness of the method. In addition, a comparative analysis was conducted with the existing prediction models, which proved that the proposed prediction model has certain superiority.

Probabilistic model of composite open-hole

The composite open-hole laminate is manufactured with carbon-fiber-reinforced composite material. The overall size of the composite open-hole laminate is 200 mm × 36 mm × 3.6 mm. A perforation with a diameter of 6 mm is located at the center of the plate, as shown in Fig. 1. The fiber layer order is [45/0/-45/90]_{2s}.

Due to the complexity of the preparation process, the mechanical properties of the composite open-hole laminates have a certain dispersion. If the factors affecting the ultimate load are taken as random variables, and the ultimate load is taken as the response value, the structural response function can be expressed as:

$$F = G(\mathbf{x}) = G(x_1, x_2, \dots, x_n) \quad (1)$$

where F is the ultimate load of $G_0 = G(\boldsymbol{\mu})\mathbf{x} = (x_1, x_2, \dots, x_n)$ open-hole laminate under $\boldsymbol{\mu} = (\mu_1, \mu_2, \dots, \mu_n)$ ensile, x_i is the random variable.

In this paper, the fiber parameters are taken as random variables, with the statistical characteristics shown in Table 1. All random variables are first assumed to follow normal distributions with setting the coefficients of variation equal to 0.05²².

Dimension reduction method

The structural response function $G(x)$ consists of n -dimensional random variable, as a continuously differentiable real-valued function, which can be expressed as a sum of lower-order functions in an increasing hierarchy²³⁻²⁵.

$$F = G(x) = G_0 + \sum_{i=1}^n G_i(x_i) + \sum_{1 \leq i < j \leq n} G_{ij}(x_i, x_j) + \dots + \sum_{1 \leq i_1 < \dots < i_k \leq n} G_{i_1 i_2 \dots i_k}(x_{i_1}, x_{i_2}, \dots, x_{i_k}) + \dots + G_{12 \dots n}(x_1, x_2, \dots, x_n) \tag{2}$$

where G_0 is the zeroth-order effect, which is a constant, and the first-order component function $G_i(x_i)$ gives the independent contribution to F by the i -th random variable acting alone, the second order component function $G_{ij}(x_i, x_j)$ gives the pair correlated contribution to F by the random variables x_i and x_j , etc. The last term $G_{12 \dots n}(x_1, x_2, \dots, x_n)$ contains any residual n -th order correlated contribution of all random variables.

Based on the theoretical method of center point dimensionality reduction²⁶, each sub-function of Eq. (2) is expanded at a specified point, and each sub-item expression after expansion is:

$$G_0 = G(\mu) \tag{3}$$

$$G_i(x_i) = G(\mu_1, \dots, \mu_{i-1}, x_i, \mu_{i+1}, \dots, \mu_n) - G_0 \tag{4}$$

$$G_{ij}(x_i, x_j) = G(\mu_1, \dots, \mu_{i-1}, x_i, \mu_{i+1}, \dots, \mu_{j-1}, x_j, \mu_{j+1}, \dots, \mu_n) - G_i(x_i) - G_j(x_j) - G_0 \tag{5}$$

$$G_{ijk}(x_i, x_j, x_k) = G(\mu_1, \mu_2, \dots, x_i, x_j, x_k, \dots, \mu_n) - G_{ij}(x_i, x_j) - G_{ik}(x_i, x_k) - G_{jk}(x_j, x_k) - G_i(x_i) - G_j(x_j) - G_k(x_k) - G_0 \tag{6}$$

$$G_{12 \dots n}(x_1, x_2, \dots, x_n) = G(x) - G_0 - \sum_{1 \leq i \leq n} G_i(x_i) - \sum_{1 \leq i < j \leq n} G_{ij}(x_i, x_j) - \dots - \sum_{1 \leq i_1 < \dots < i_{n-1} \leq n} G_{i_1 i_2 \dots i_{n-1}}(x_{i_1}, x_{i_2}, \dots, x_{i_{n-1}}) \tag{7}$$

Where $G(\mu) = G(\mu_1, \mu_2, \dots, \mu_n)$ is a constant calculated at the mean value of each random variable.

For a continuously differentiable function, the calculated value of the higher-order terms of Eq. (2) is much smaller than the lower-order terms and can be ignored. Therefore, the function in Eq. (2) is only reserved for the first-order item. The univariate dimensionality reduction expression of the structural response function is obtained as:

$$F = G(x_1, x_2, \dots, x_n) \cong \sum_{i=1}^n G(x_i) - (n - 1)G_0 \tag{8}$$

By transforming the n -dimensional function into the sum of one-dimensional functions, the computational cost of the structural response function is effectively reduced.

Univariate legendre approximate model

The first-order function $G(x_i)$ of Eq. (8) can be represented by LP. Since LP is included in $[-1, 1]$, the value of random variable x_i are first determined according to the three-sigma (3σ) rule²⁷: $x_i \in [a_i, b_i]$, $a_i = \mu_i - 3\sigma_i$, $b_i = \mu_i + 3\sigma_i$, ($i = 1, 2, \dots, n$), where μ_i is the mean value of x_i , and σ_i is the standard deviation of x_i . The variable $x_i \in [a_i, b_i]$ is converted to $[-1, 1]$, by the following expression:

$$t_i = \frac{2x_i - (a_i + b_i)}{b_i - a_i}, i = 1, 2, \dots, n \tag{9}$$

For univariate function $G(x_i)$, $x_i \in [a_i, b_i]$, Using LP to approximate $G(x_i)$, the ULAM can be obtained as²⁸:

$$G(x_i) \approx f(t_i) = \sum_{j=0}^k C_{ij} L_j(t_i) \tag{10}$$

where C_{ij} denotes LP coefficients, $L_j(t_i)$ is LP.

If $L_n(t)$ is used to represent the n -dimensional LP, $L_n(t)$ can be defined as:

$$L_n(t) = \frac{n!}{(2n)!} \frac{d^n (t^2 - 1)^n}{dt^n} \tag{11}$$

The recurrence relation of LP can be written as:

$$L_1(t) = 1 \tag{12}$$

$$L_2(t) = t \tag{13}$$

⋮

$$L_{n+1}(t) = \frac{2n+1}{n+1}tL_n(t) - \frac{n}{n+1}L_{n-1}(t) \tag{14}$$

C_{ij} can be calculated by the Gauss-Legendre integration formula²⁹:

$$C_{i,j} = \frac{2n+1}{2} \int_{-1}^1 L_n(t) f(t) dt = \frac{2n+1}{2} \sum_{l=1}^m A_l L_n(t_l) f(t_l) \tag{15}$$

$$A_l = \int_{-1}^1 \frac{L_m(t)}{(t-t_l)L'_l(t_l)} dt = \frac{2}{(1-t_l^2)[L'_l(t_l)]^2}, l = 1, 2, \dots, m \tag{16}$$

where m is the number of interpolation points ($m = n + 1$), t_l is interpolation point, and $f(t)$ is the ultimate load value at the interpolation point. The interpolation points are the zeros of the LP of degree $n + 1$. The structural response of the interpolation points is obtained through finite element calculation.

The ULAM of the response function can be obtained as:

$$F = G(x_1, x_2, \dots, x_n) \cong \sum_{i=1}^n \sum_{j=0}^k C_{ij} L_j(t_i) - (n-1)G_0 \tag{17}$$

The computational algorithm for the ULAM is show as Fig. 2.

Finite element analysis

Composite open-hole laminates are modeled with 3D solids, and each layer is individually given material orientation according to the layer order. The finite element model of composite open-hole laminate is shown as Fig. 3. The mesh is refined for the open-hole part to improve the accuracy of the calculation results, and the mesh type is a 3D solid linear reduction integration unit (C3D8R). One end of the laminate is fixed, and the other end is loaded with displacement load, and the loading displacement is 10 mm.

It is analyzed for progressive damage by ABAQUS/Explicit. Based on 3D Hashin damage initiation criterion^{30,31} and Chang-Chang damage extension criterion³², a user subroutine for ABAQUS is written to calculate the tension strength of composite open-hole laminate.

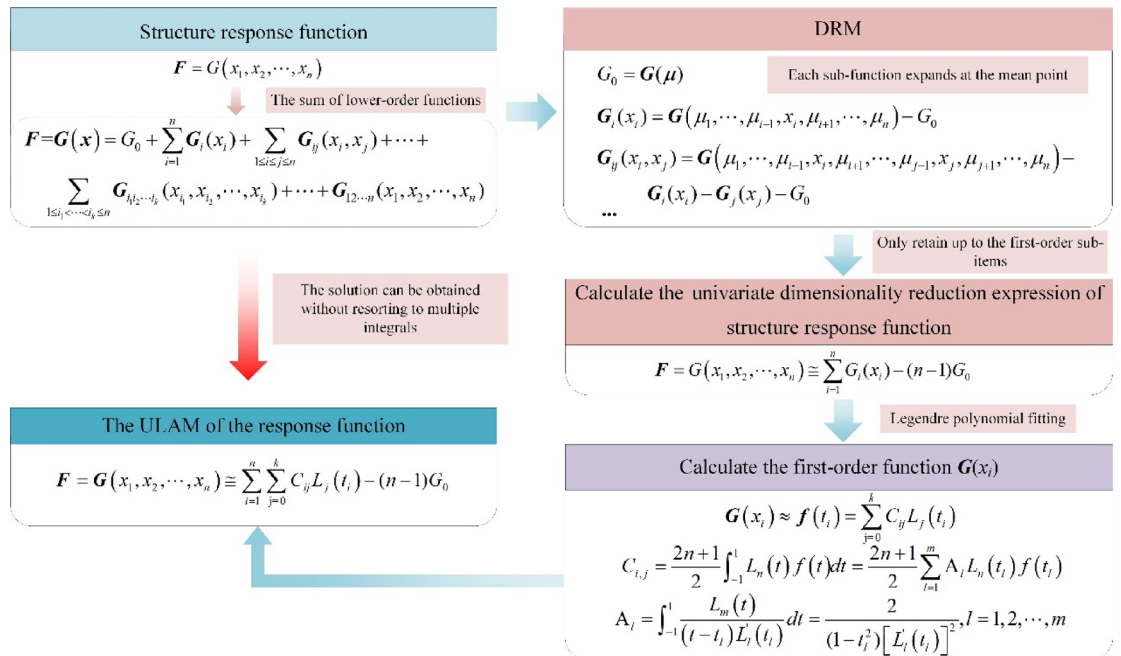


Fig. 2. Computational algorithm.

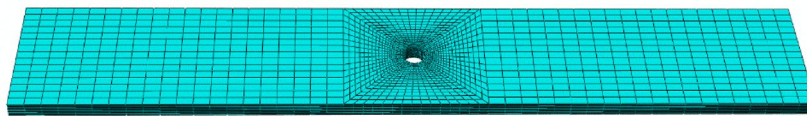


Fig. 3. Finite element model of composite open-hole laminate.

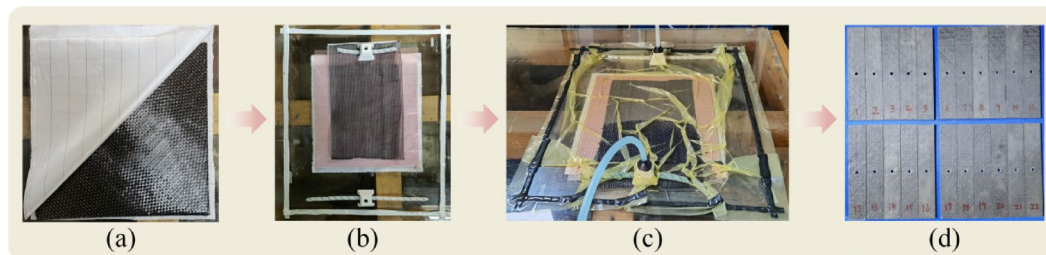


Fig. 4. Manufacture of composite laminate.

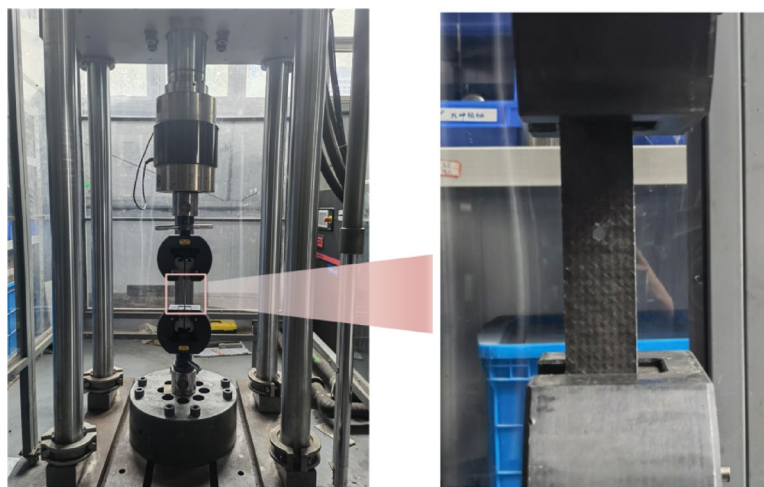


Fig. 5. Experimental device.

Specimens and experiments

Sample Preparation

In order to conduct experimental research on the probabilistic strength of composite open-hole laminate and further verify the correctness of the proposed probabilistic model, 22 samples were made with reference to ASTM D 5766/D 5766 M-11.

The composite laminate is made of T300 carbon fiber unidirectional cloth and epoxy vinyl resin. The preparation process is vacuum assistant resin infusion process (VARI), as shown in Fig. 4 (a)-(c). The prepared composite laminates were subjected to hole-opening, and the final samples obtained are shown in Fig. 4 (d).

Experimental method

The composite open-hole panels were subjected to tensile tests using an MTS 311.32 testing machine (MTS System Corp, Eden Prairie, MN, USA) to obtain the tensile strength. The loading method is displacement loading, and the loading speed is 1 mm/min. The sample is clamped as shown in Fig. 5.

Results and discussion

Model validation

Static tension experiments were conducted on twenty-two composite open-hole laminates, and the ultimate loads value are shown in Fig. 6; Table 2. The mean value and standard deviation of the ultimate loads are 46.349kN and 2.764kN, respectively.

Figure 7 shows the comparisons of predicted and experimental CDF. The results show that the experimental test results are all quite near to the expected curves. Among these, the prediction curves derived using ULAM

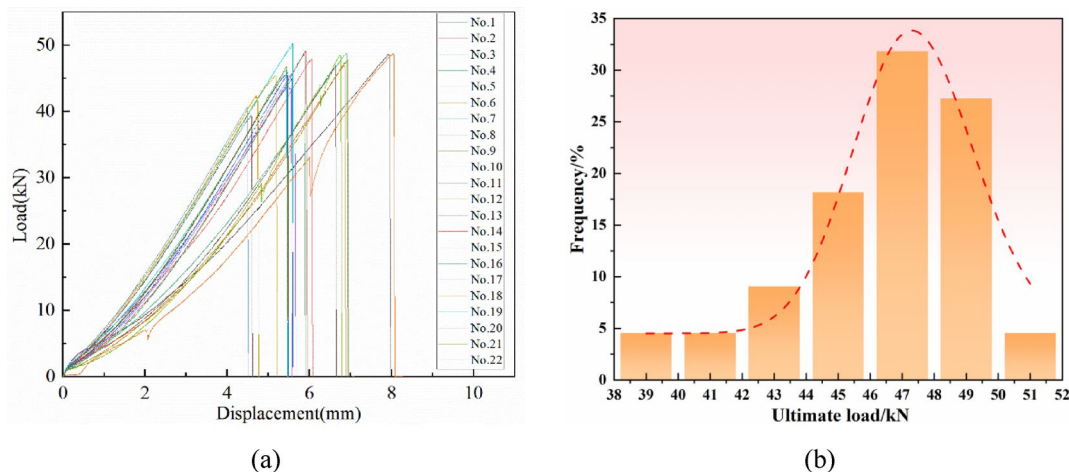


Fig. 6. Static tension experimental results. (a) Load-displacement curves of composite open-hole laminate, (b) The ultimate loads distribution of composite open-hole laminate.

no.	Ultimate load/kN	no.	Ultimate load/kN	no.	Ultimate load/kN	no.	Ultimate load/kN
1	48.642	7	46.329	13	45.871	19	50.282
2	47.871	8	46.963	14	49.176	20	39.514
3	45.014	9	46.807	15	45.446	21	47.771
4	48.776	10	46.963	16	48.694	22	48.687
5	43.925	11	40.595	17	46.098		
6	45.383	12	48.472	18	42.404		

Table 2. Experimental results for the composite open-hole laminate.

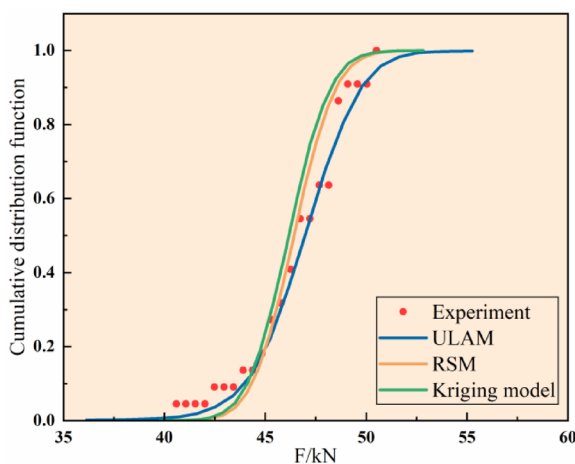


Fig. 7. Comparisons of predicted and experimental CDF.

are more similar to the experimental data. Table 3 compares the mean and standard deviation forecast findings with experimental data. The mean prediction errors for all three models are less than 3%, with the Kriging model having the least prediction error and ULAM having the greatest prediction error. In terms of the coefficient of variation (CV), the ULAM model achieves the lowest prediction error at 14.88%, while both the RSM and Kriging models exhibit errors exceeding 40%. Furthermore, the order selected by ULAM is 6. There are 77 sample points required. With the same amount of sample points, a full comparison of the three models' prediction errors reveals that ULAM has a greater prediction accuracy than the other two models. As a result, the approach presented in this study may be used to reliably forecast the mean and CV of the ultimate load of composite open-hole laminates.

	Experiment	ULAM		RSM		Kriging model	
		Predict	Error/%	Predict	Error/%	Predict	Error/%
μ_F /kN	46.349	47.350	2.16	46.708	0.77	46.485	0.29
CV (%)	5.963	5.076	14.88	3.490	41.47	3.488	41.52
Sample point	/	77		77		77	

Table 3. Errors of the mean values and standard deviations for the prediction results. Where μ_F is mean, CV is coefficient of variation.

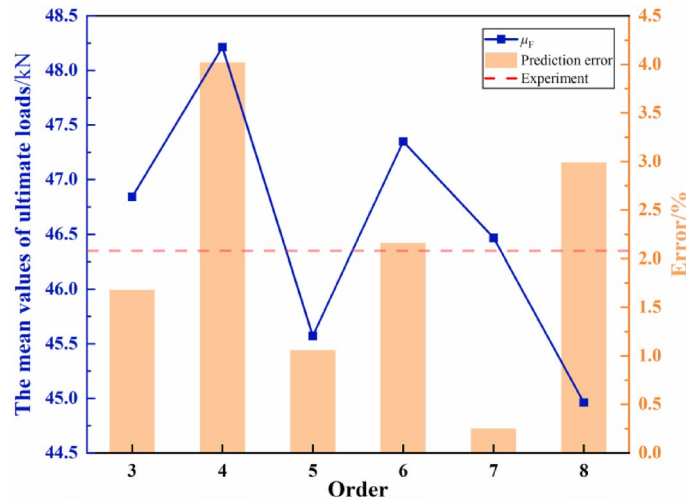


Fig. 8. Comparison of mean value prediction accuracy for different orders.

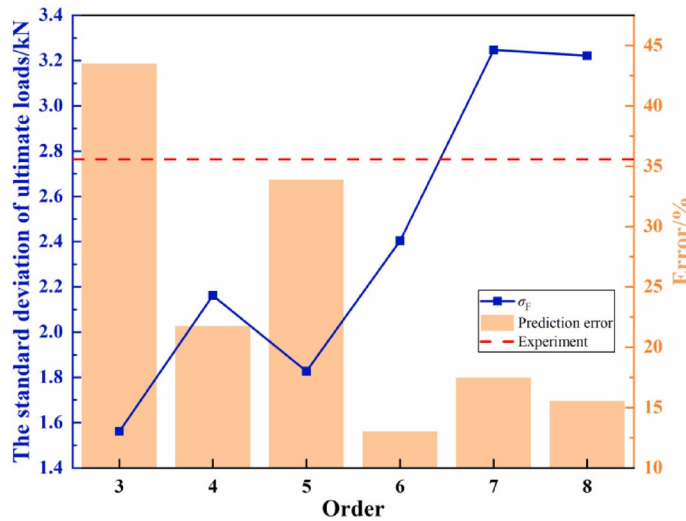


Fig. 9. Comparison of standard deviation prediction accuracy for different orders.

Influence of order on the accuracy of ULAM

Since the order of ULAM will affect the fitting accuracy, the effect of different orders (3th-8th) on the prediction accuracy was explored.

Figures 8 and 9 show the comparison of the prediction results of ULAM with different orders for mean and variance, respectively. According to Figs. 8 and 9, it can be seen that the order of ULAM has a non-monotonic effect on the prediction accuracy, and the prediction errors of the mean and variance show an overall trend of decreasing and then increasing as the order increases. When the order is low (3th-4th), the prediction effect of the ULAM is poor, indicating that too low order will lead to underfitting. When the order of ULAM is greater than 4, the prediction accuracy of ULAM increases with increasing order. That is, the increase in the number

P	Experiment	Order											
		3		4		5		6		7		8	
		P	E/%	P	E/%	P	E/%	P	E/%	P	E/%	P	E/%
μ_F /kN	46.349	45.571	1.68	48.214	4.02	46.842	1.06	47.350	2.16	44.961	0.25	30.942	2.99
σ_F /kN	2.764	1.5617	43.50	2.1621	21.78	1.8268	33.91	2.4036	13.04	3.2221	17.49	3.8876	15.57
Sample point	/	45		55		67		77		89		99	

Table 4. The prediction accuracy comparison of different orders. Where P is Predict, E is Error.

of sample points can improve the prediction accuracy of ULAM. If the order is too high (8th), overfitting will occur, resulting in a decline in the prediction accuracy of the ULAM. That is, high order polynomials can lead to overfitting, resulting in poorer generalization of the predictive model.

Table 4 presents a comparison of the prediction accuracy of different orders. According to Table 4, the increase of order for ULAM will improve the prediction accuracy of the model. However, the increase in order leads to an increase in the number of computational sample points, which results in a huge computational cost. For example, when the order of ULAM is increased from 6th to 7th, the prediction accuracy of the model has some improvement, but the improvement is limited, on the contrary, the computational cost increases by 16%. Therefore, it is essential to select an appropriate order to solve the uncertainty problem of composite open-hole laminate.

Conclusions

A probabilistic failure load prediction method for composite open-hole laminate was proposed combining the dimension reduction method and Legendre polynomial. The predicted results were compared with the experimental results to verify the effectiveness of the method. And it is compared with two commonly used agent models to verify the superiority of the model. The errors of the results are all less than 15%, indicating the new method can effectively predict the ultimate load value of composite open-hole laminate with probability. The fitting accuracy of ULAM is related to the order. If the order is too low, underfitting will occur. Increasing the order can improve the prediction accuracy of ULAM. If the order is too high, overfitting will occur, resulting in a decline in the prediction accuracy of the model. In the process of practical application of engineering, it is necessary to take into account the calculation accuracy and calculation cost and reasonably select the order of ULAM.

Data availability

All data generated or analysed during this study are included in this published article.

Received: 19 June 2025; Accepted: 23 December 2025

Published online: 30 December 2025

References

- Li, H., Tu, S., Liu, Y., Lu, X. & Zhu, X. Mechanical properties of L-joint with composite sandwich structure. *Compos. Struct.* **217**, 165–174 (2019).
- Liu, Y., Li, M., Lu, X. & Zhu, X. Failure mechanism and strength prediction model of T-joint of composite sandwich structure. *Metals*. **11**. (2021).
- Delbariani-Nejad, A., Farrokhhabadi, A. & Jafari, R. S. An energy based approach for reliability analysis of delamination growth under mode I, mode II and mixed mode I/II loading in composite laminates. *Int. J. Mech. Sci.* **145**. (2018).
- Chiachio, M., Chiachio, J. & Rus, G. Reliability in composites – A selective review and survey of current development. *Compos. Part. B: Eng.* **43**, 902–913 (2012).
- Delbariani-Nejad, A., Farrokhhabadi, A. & Fotouhi, M. Finite element reliability analysis of edge delamination onset due to interlaminar stresses in composite laminates. *Compos. Struct.* **115410**, 288 (2022).
- Omairey, S. L., Dunning, P. D. & Sriramula, S. Multi-scale reliability-based design optimisation framework for fibre-reinforced composite laminates. *Eng. Comput.* **38**, 1241–1262 (2020).
- Delbariani-Nejad, A., Farrokhhabadi, A. & Fotouhi, M. Propose a generic framework for probabilistic prediction of the onset and growth of matrix cracking induced delamination in composite laminates. *Eng. Fract. Mech.* **108262**, 261 (2022).
- Delbariani-Nejad, A. & Xiong, Y. Probabilistic investigation of piezoelectric application for reliability enhancement of composite laminates under edge delamination. *Compos. Struct.* **118528**, 346–350 (2024).
- Wan, A., Li, D. & Lu, P. C. Three-scale modeling and probabilistic progressive damage analysis of woven composite laminates. *Mech. Adv. Mater. Struct.* **31**, 602–618 (2022).
- Lubritz, J., Krimmer, A. & Bardenhagen, A. Characterization of a carbon fiber-reinforced polymer by a probabilistic simulation approach using micromechanical modeling. *Mech. Compos. Mater.* **61**, 319–334 (2025).
- Tang, X. Probabilistic analysis for the pre-stressed vibratory characteristics of composite fan blades based on a forward uncertainty propagation. *Proceedings of the institution of mechanical engineers part c-journal of mechanical engineering science.* **239**, 7038–7057. (2025).
- Mukherjee, S., Ganguli, R. & Gopalakrishnan, S. Optimization of laminated composite structure considering uncertainty effects. *Mech. Adv. Mater. Struct.* **26**, 493–502 (2017).
- Lin, S. C. & Kam, T. Y. Probabilistic failure analysis of transversely loaded laminated composite plates using first-order second moment method. *J. Eng. Mech.* **126**, 812–820 (2000).
- Davidson, P. & Waas, A. M. Probabilistic defect analysis of fiber reinforced composites using kriging and support vector machine based surrogates. *Compos. Struct.* **195**, 186–198 (2018).
- Zhou, C., Li, C., Zhang, H., Zhao, H. & Zhou, C. Reliability and sensitivity analysis of composite structures by an adaptive Kriging based approach. *Composite Structures.* **278**. (2021).

16. Haeri, A. & Fadaee, M. J. Efficient reliability analysis of laminated composites using advanced kriging surrogate model. *Compos. Struct.* **149**, 26–32 (2016).
17. Patel, S. & Guedes Soares, C. Reliability assessment of glass epoxy composite plates due to low velocity impact. *Compos. Struct.* **200**, 659–668 (2018).
18. Patel, S. & Guedes Soares, C. System probability of failure and sensitivity analyses of composite plates under low velocity impact. *Compos. Struct.* **180**, 1022–1031 (2017).
19. Carrere, N., Rollet, Y., Leroy, F. H. & Maire, J. F. Efficient structural computations with parameters uncertainty for composite applications. *Compos. Sci. Technol.* **69**, 1328–1333 (2009).
20. Li, F., Li, H., Zhao, H. & Zhou, Y. A dimension-reduction based Chebyshev polynomial method for uncertainty analysis in composite corrugated sandwich structures. *J. Compos. Mater.* **56**, 1891–1900 (2022).
21. Li, X., Lv, Z. & Qiu, Z. A novel univariate method for mixed reliability evaluation of composite laminate with random and interval parameters. *Compos. Struct.* **203**, 153–163 (2018).
22. Li, H.-S. Maximum entropy method for probabilistic bearing strength prediction of pin joints in composite laminates. *Compos. Struct.* **106**, 626–634 (2013).
23. Li, G., Rosenthal, C. & Rabitz, H. High dimensional model representations. *J. Phys. Chem. A.* **105**, 7765–7777 (2001).
24. Rabitz, H. & Ali, M. F. General foundations of high dimensional model representations. *J. Math. Chem.* **25**, 197–233 (1999).
25. Rahman, S. & Xu, H. A univariate dimension-reduction method for multi-dimensional integration in stochastic mechanics. *Probab. Eng. Mech.* **19**, 393–408 (2004).
26. Rahman, S. A polynomial dimensional decomposition for stochastic computing. *Int. J. Numer. Methods Eng.* **76**, 2091–2116 (2010).
27. Jeong, J. et al. Identifying outliers of non-Gaussian groundwater state data based on ensemble Estimation for long-term trends. *J. Hydrol.* **548**, 135–144 (2017).
28. Feng, X., Zhang, Y. & Wu, J. Interval analysis method based on legendre polynomial approximation for uncertain multibody systems. *Adv. Eng. Softw.* **121**, 223–234 (2018).
29. Press, W. H., Teukolsky, S. A., Vetterling, W. T. & Flannery, B. P. Numerical recipes. In *The Art of Scientific Computing* (Cambridge University Press, 2007).
30. Hashin, Z. Fatigue failure criteria for unidirectional fiber composites. *Journal Appl. Mechanics* (1981).
31. Braun, M. & Ariza, M. P. New lattice models for dynamic fracture problems of anisotropic materials. *Compos. Part. B: Eng.* **172**, 760–768 (2019).
32. Chang, F. K. & Chang, K. Y. A progressive damage model for laminated composites containing stress concentrations. *J. Compos. Mater.* **21**, 834–855 (1987).

Acknowledgements

We greatly appreciate the financial support from National Major Scientific Research Instrument Development Program of China (No. 12027901).

Author contributions

Conceptualization, M.L.; methodology, M.L.; software, M.L.; supervision, X.Z.; validation, F.L.; visualization, F.L.; writing—original draft, M.L.; writing—review and editing, X.Z. All authors have read and agreed to the published version of the manuscript.

Funding

This research was funded by the National key research and development program of China (No. 2022YFB3707104).

Declarations

Competing interests

The authors declare no competing interests.

Additional information

Correspondence and requests for materials should be addressed to X.Z.

Reprints and permissions information is available at www.nature.com/reprints.

Publisher's note Springer Nature remains neutral with regard to jurisdictional claims in published maps and institutional affiliations.

Open Access This article is licensed under a Creative Commons Attribution-NonCommercial-NoDerivatives 4.0 International License, which permits any non-commercial use, sharing, distribution and reproduction in any medium or format, as long as you give appropriate credit to the original author(s) and the source, provide a link to the Creative Commons licence, and indicate if you modified the licensed material. You do not have permission under this licence to share adapted material derived from this article or parts of it. The images or other third party material in this article are included in the article's Creative Commons licence, unless indicated otherwise in a credit line to the material. If material is not included in the article's Creative Commons licence and your intended use is not permitted by statutory regulation or exceeds the permitted use, you will need to obtain permission directly from the copyright holder. To view a copy of this licence, visit <http://creativecommons.org/licenses/by-nc-nd/4.0/>.

© The Author(s) 2026